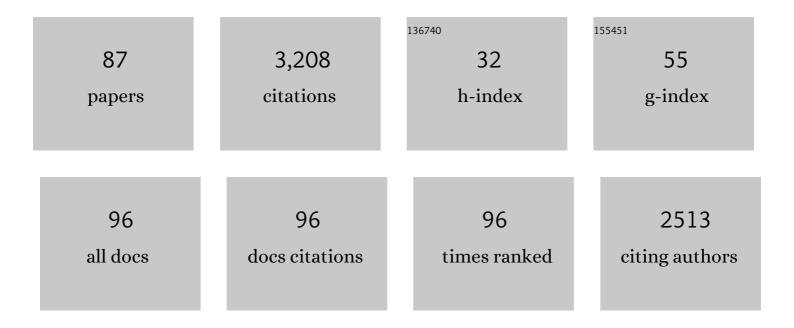
Trond M Ryberg

List of Publications by Year in descending order

Source: https://exaly.com/author-pdf/1019237/publications.pdf Version: 2024-02-01



TROND M RVREDC

#	Article	IF	CITATIONS
1	Dynamic strain determination using fibre-optic cables allows imaging of seismological and structural features. Nature Communications, 2018, 9, 2509.	5.8	360
2	Receiver function arrays: a reflection seismic approach. Geophysical Journal International, 2000, 141, 1-11.	1.0	168
3	P-wave mantle velocity structure beneath northern Eurasia from long-range recordings along the profile Quartz. Physics of the Earth and Planetary Interiors, 1993, 79, 269-286.	0.7	119
4	The crustal structure of the Dead Sea Transform. Geophysical Journal International, 2004, 156, 655-681.	1.0	107
5	Structure of the California Coast Ranges and San Andreas Fault at SAFOD from seismic waveform inversion and reflection imaging. Journal of Geophysical Research, 2007, 112, .	3.3	102
6	Crustal structure and tectonics from the Los Angeles basin to the Mojave Desert, southern California. Geology, 2001, 29, 15.	2.0	99
7	Lake Toba volcano magma chamber imaged by ambient seismic noise tomography. Geophysical Research Letters, 2010, 37, .	1.5	90
8	Observation of high-frequency teleseismicPnon the long-range Quartz profile across northern Eurasia. Journal of Geophysical Research, 1995, 100, 18151-18163.	3.3	89
9	A natural and controlled source seismic profile through the Eastern Alps: TRANSALP. Earth and Planetary Science Letters, 2004, 225, 115-129.	1.8	89
10	DEEP CRUSTAL PROFILE ACROSS THE SOUTHERN KAROO BASIN AND BEATTIE MAGNETIC ANOMALY, SOUTH AFRICA: AN INTEGRATED INTERPRETATION WITH TECTONIC IMPLICATIONS. South African Journal of Geology, 2011, 114, 265-292.	0.6	82
11	Wave propagation in a multiple-scattering upper mantle-observations and modelling. Geophysical Journal International, 1996, 127, 492-502.	1.0	81
12	Precise location of San Andreas Fault tremors near Cholame, California using seismometer clusters: Slip on the deep extension of the fault?. Geophysical Research Letters, 2009, 36, .	1.5	78
13	Lithology-derived structure classification from the joint interpretation of magnetotelluric and seismic models. Geophysical Journal International, 2007, 170, 737-748.	1.0	75
14	Fault systems of the 1971 San Fernando and 1994 Northridge earthquakes, southern California: Relocated aftershocks and seismic images from LARSE II. Geology, 2003, 31, 171.	2.0	68
15	The Fine Structure of the Subducted Investigator Fracture Zone in Western Sumatra as Seen by Local Seismicity. Earth and Planetary Science Letters, 2010, 298, 47-56.	1.8	64
16	New "Fresnel-Zone―estimates for shear-wave splitting observations from finite-difference modeling. Geophysical Research Letters, 2000, 27, 2005-2008.	1.5	63
17	Boundary-layer mantle flow under the Dead Sea transform fault inferred from seismic anisotropy. Nature, 2003, 425, 497-501.	13.7	61
18	The crustal structure beneath the Central Andean forearc and magmatic arc as derived from seismic studies — the PISCO 94 experiment in northern Chile (21°–23°S). Journal of South American Earth Sciences, 1999, 12, 237-260.	0.6	58

#	Article	IF	CITATIONS
19	Anatomy of the Dead Sea Transform from lithospheric to microscopic scale. Reviews of Geophysics, 2009, 47, .	9.0	56
20	South Atlantic opening: A plume-induced breakup?. Geology, 2015, 43, 931-934.	2.0	54
21	Geophysical images of the Dead Sea Transform in Jordan reveal an impermeable barrier for fluid flow. Geophysical Research Letters, 2003, 30, .	1.5	53
22	The San Gabriel Mountains bright reflective zone: possible evidence of young mid-crustal thrust faulting in southern California. Tectonophysics, 1998, 286, 31-46.	0.9	49
23	Structure of the San Andreas fault zone at SAFOD from a seismic refraction survey. Geophysical Research Letters, 2006, 33, .	1.5	48
24	Modeling of seismic guided waves at the Dead Sea Transform. Journal of Geophysical Research, 2003, 108, .	3.3	47
25	Southern African continental margin: Dynamic processes of a transform margin. Geochemistry, Geophysics, Geosystems, 2009, 10, .	1.0	46
26	Finite difference modelling of P-wave scattering in the upper mantle. Geophysical Journal International, 2000, 141, 787-800.	1.0	44
27	High-frequency wave propagation in the uppermost mantle. Journal of Geophysical Research, 1999, 104, 10655-10666.	3.3	43
28	AcehSeis project provides insights into the detailed seismicity distribution and relation to fault structures in Central Aceh, Northern Sumatra. Journal of Asian Earth Sciences, 2019, 171, 20-27.	1.0	40
29	Crustal structure of the eastern Dabie Shan interpreted from deep reflection and shallow tomographic data. Tectonophysics, 2001, 333, 347-359.	0.9	39
30	Initial results from wide-angle seismic refraction lines in the southern Cape. South African Journal of Geology, 2007, 110, 407-418.	0.6	37
31	Deep Crustal Seismic Reflection Experiment Across the Southern Karoo Basin, South Africa. South African Journal of Geology, 2007, 110, 419-438.	0.6	37
32	Scales of Heterogeneities in the Continental Crust and Upper Mantle. Pure and Applied Geophysics, 1999, 156, 29-52.	0.8	35
33	Crustal structure of the southern margin of the African continent: Results from geophysical experiments. Journal of Geophysical Research, 2008, 113, .	3.3	32
34	Crustal structure of northwest Namibia: Evidence for plume-rift-continent interaction. Geology, 2015, 43, 739-742.	2.0	31
35	Shallow architecture of the Wadi Araba fault (Dead Sea Transform) from high-resolution seismic investigations. Tectonophysics, 2007, 432, 37-50.	0.9	30
36	Upper Crustal Structure from the Santa Monica Mountains to the Sierra Nevada, Southern California: Tomographic Results from the Los Angeles Regional Seismic Experiment, Phase II (LARSE II). Bulletin of the Seismological Society of America, 2004, 94, 619-632.	1.1	29

#	Article	IF	CITATIONS
37	Characterizing a large shear-zone with seismic and magnetotelluric methods: The case of the Dead Sea Transform. Geophysical Research Letters, 2005, 32, .	1.5	29
38	Images of crust beneath southern California will aid study of earthquakes and their effects. Eos, 1996, 77, 173-176.	0.1	27
39	Short-period observation of the 520 km discontinuity in northern Eurasia. Journal of Geophysical Research, 1997, 102, 5413-5422.	3.3	27
40	Submarine permafrost depth from ambient seismic noise. Geophysical Research Letters, 2015, 42, 7581-7588.	1.5	27
41	Properties of the mantle transition zone in northern Eurasia. Journal of Geophysical Research, 1998, 103, 811-822.	3.3	25
42	Classification of lithology from seismic tomography: A case study from the Messum igneous complex, Namibia. Journal of Geophysical Research, 2003, 108, .	3.3	24
43	Upper mantle anisotropy beneath the Seychelles microcontinent. Journal of Geophysical Research, 2005, 110, .	3.3	24
44	Imaging the Dead Sea Transform with scattered seismic waves. Geophysical Journal International, 2004, 158, 179-186.	1.0	22
45	Simultaneous inversion of shear wave splitting observations from seismic arrays. Journal of Geophysical Research, 2005, 110, .	3.3	22
46	Locating non-volcanic tremor along the San Andreas Fault using a multiple array source imaging technique. Geophysical Journal International, 2010, 183, 1485-1500.	1.0	22
47	Body wave observations from cross-correlations of ambient seismic noise: A case study from the Karoo, RSA. Geophysical Research Letters, 2011, 38, n/a-n/a.	1.5	22
48	Anatomy of a crustal-scale accretionary complex: Insights from deep seismic sounding of the onshore western Makran subduction zone, Iran. Geology, 2021, 49, 3-7.	2.0	21
49	The onset of Walvis Ridge: Plume influence at the continental margin. Tectonophysics, 2017, 716, 90-107.	0.9	20
50	Rapid continental breakup and microcontinent formation in the western Indian Ocean. Eos, 2004, 85, 481.	0.1	19
51	Uppermost mantle and crustal structure at Tristan da Cunha derived from ambient seismic noise. Earth and Planetary Science Letters, 2017, 471, 117-124.	1.8	18
52	The wide-angle seismic image of a complex rifted margin, offshore North Namibia: Implications for the tectonics of continental breakup. Tectonophysics, 2017, 716, 130-148.	0.9	18
53	Subsurface Geometry of the San Andreas Fault in Southern California: Results from the Salton Seismic Imaging Project (SSIP) and Strong Ground Motion Expectations. Bulletin of the Seismological Society of America, 0, , .	1.1	18
54	Seismic mapping of shallow fault zones in the San Gabriel Mountains from the Los Angeles Region Seismic Experiment, southern California. Journal of Geophysical Research, 2001, 106, 6549-6568.	3.3	17

#	Article	IF	CITATIONS
55	Bayesian inversion of refraction seismic traveltime data. Geophysical Journal International, 2018, 212, 1645-1656.	1.0	17
56	The shallow velocity structure across the Dead Sea Transform fault, Arava Valley, from seismic data. Journal of Geophysical Research, 2007, 112, .	3.3	16
57	Lithology classification from seismic tomography: Additional constraints from surface waves. Journal of African Earth Sciences, 2010, 58, 547-552.	0.9	14
58	Ambient seismic noise tomography reveals a hidden caldera and its relation to the Tarutung pull-apart basin at the Sumatran Fault Zone, Indonesia. Journal of Volcanology and Geothermal Research, 2016, 321, 73-84.	0.8	14
59	Multinational geoscientific research effort kicks off in the Middle East. Eos, 2000, 81, 609-617.	0.1	13
60	Tomographic Vp and Vs structure of the California Central Coast Ranges, in the vicinity of SAFOD, from controlled-source seismic data. Geophysical Journal International, 2012, 190, 1341-1360.	1.0	12
61	Global Significance of a Sub-Moho Boundary Layer (SMBL) Deduced from High-Resolution Seismic Observations. International Geology Review, 2002, 44, 671-685.	1.1	10
62	Bayesian simultaneous inversion for local earthquake hypocentres and 1-D velocity structure using minimum prior knowledge. Geophysical Journal International, 2019, 218, 840-854.	1.0	10
63	Seismic Imaging of the Waltham Canyon Fault, California: Comparison of Rayâ€Theoretical and Fresnel Volume Prestack Depth Migration. Bulletin of the Seismological Society of America, 2013, 103, 340-352.	1.1	9
64	Relocation of earthquakes in the southern and eastern Alps (Austria, Italy) recorded by the dense, temporary SWATH-D network using a Markov chain Monte Carlo inversion. Solid Earth, 2021, 12, 1087-1109.	1.2	9
65	Results of geophysical studies across the Dead Sea Transform: The Arava/Araba Valley and the Dead Sea Basin. Israel Journal of Earth Sciences, 2009, 58, 147-161.	0.3	9
66	Detailed P- and S-Wave Velocity Models along the LARSE II Transect, Southern California. Bulletin of the Seismological Society of America, 2010, 100, 3194-3212.	1.1	8
67	Shallow seismic velocity structure of the Karoo Basin, South Africa. South African Journal of Geology, 2007, 110, 439-448.	0.6	7
68	Ambient seismic noise analysis of LARGE-N data for mineral exploration in the Central Erzgebirge, Germany. Solid Earth, 2022, 13, 519-533.	1.2	7
69	Shallow lithological structure across the Dead Sea Transform derived from geophysical experiments. Geochemistry, Geophysics, Geosystems, 2011, 12, n/a-n/a.	1.0	6
70	Observation of teleseismic P n/S n on super long-range profiles in northern Eurasia and their implications for the structure of the lithosphere. , 1997, , 63-73.		5
71	Survey yields data on unique metamorphic rock complex in China. Eos, 1998, 79, 429-429.	0.1	4

52 Small-Scale Heterogeneities of the Upper Mantle. , 1997, , 215-223.

4

#	Article	IF	CITATIONS
73	Seismic Detection Limits of Small, Deep, Man-Made Reflectors: A Test at a Geothermal Site in Northern Germany. Bulletin of the Seismological Society of America, 2005, 95, 1567-1573.	1.1	3
74	Nearâ€surface properties of an active fault derived by joint interpretation of different geophysical methods ―the Arava/Araba Fault in the Middle East. Near Surface Geophysics, 2012, 10, 381-390.	0.6	3
75	The shallow P-velocity structure of the southern Dead Sea basin derived from near-vertical incidence reflection seismic data in project DESIRE. Geophysical Journal International, 2012, 188, 524-534.	1.0	3
76	Finite difference modelling of elastic wave propagation in the Earth's uppermost mantle. , 2000, , 3-12.		3
77	Finite Difference Modelling of Seismic Wave Phenomena within the Earth's Upper Mantle. , 2001, , 48-56.		2
78	Geophysical Studies of the Lithosphere Along the Dead Sea Transform. Modern Approaches in Solid Earth Sciences, 2014, , 29-52.	0.1	2
79	Correction to "Anatomy of the Dead Sea Transform from lithospheric to microscopic scaleâ€. Reviews of Geophysics, 2010, 48, .	9.0	1
80	Upper mantle structure at Walvis Ridge from P n tomography. Tectonophysics, 2017, 716, 121-129.	0.9	1
81	A Fast GUI-Based Tool for Group-Velocity Analysis of Surface Waves. Seismological Research Letters, 2021, 92, 2640-2646.	0.8	1
82	Crustal and uppermost mantle structure of the NW Namibia continental margin and the Walvis Ridge derived from ambient seismic noise. Geophysical Journal International, 2022, 230, 377-391.	1.0	1
83	A new approach to describe the seismic wavefield using higher order Gaussian beam modes. Geophysical Journal International, 1991, 105, 619-628.	1.0	0
84	New insights into the seismic time term method for heterogeneous upper mantle slowness structures. GEM - International Journal on Geomathematics, 2017, 8, 43-56.	0.7	0
85	Finite-Difference Simulations of Seismic Wavefields in Isotropic and Anisotropic Earth Models. , 2002, , 35-47.		0
86	Heterogeneity of the Uppermost Mantle Inferred From Controlled-Source Seismology. , 2003, , 281-297.		0
87	Scales of Heterogeneities in the Continental Crust and Upper Mantle. , 1999, , 29-52.		0